

Modelling the Effects of Farnesol and CO₂ on the cAMP Pathway Regulating Morphogenesis in *Candida albicans*

Mareta W. Ardyani

Abstract— *Candida albicans* is reported to be the predominant cause of invasive fungal infections. Morphogenesis is named as one of the main factors making this organism an effective pathogen. Among several different signaling cascades governing morphogenesis in *C. albicans*, the cAMP pathway is reported to be the most crucial, with most signals being regulated through the adenylyl cyclase, Cyr1p. Here we present two mathematical models which investigate the roles of a quorum sensing molecule, farnesol, in inhibiting the cAMP pathway and CO₂ in activating it: Model 1, where farnesol directly degrades cAMP and Model 2, where farnesol triggers the dissociation of the complex Cyr1p-CO₂, a vital agent in cAMP production. Throughout our analysis, we demonstrate that Model 2 performs a more effective mechanism in inhibiting the cAMP pathway compared to that of Model 1. Finally, we suggest that if we could design a therapeutic molecule to treat fungal infections caused by *C. albicans*, the molecule should target Cyr1p~CO₂ instead of cAMP.

Index Terms— cAMP pathway, *Candida albicans*, farnesol, modelling, morphogenesis

I. INTRODUCTION

Candida albicans: a commensal or a pathogen?

Among the currently known human fungal pathogens, *Candida albicans* is the best studied and the most commonly found [1]. This fungus belongs to the genus *Candida*, and is believed to be the main cause of candidiasis or widely known as thrush (technically known as candidosis). It is an opportunistic fungal pathogen that resides in the gastrointestinal, vaginal and oral tracts, and skin. It is usually considered to be part of the normal flora of healthy individuals, being a harmless commensal. Under certain host-conditions, this species can turn into a pathogen causing diseases ranging from mucosal infections which are usually not life-threatening to systemic infections associated with high mortality rates [1, 2, 3, 4]. To transform from a harmless commensal into a hyper-virulent pathogen in the susceptible host, *C. albicans* can go through a series of virulence determinants including the secretion of aspartyl proteinases, adherence to mucosal surfaces, hyphal formation, thigmotropism and phenotype switching (see [5] for a review of this).

Like other *Candida* species, to act as a pathogen *C. albicans* needs to interrupt normal host defenses. Common risk factors for *C. albicans* infections include immunocompromised status, diabetes mellitus, and iatrogenic factors like antibiotic use, indwelling devices, intravenous drug use, and hyperalimentation fluids [6].

Mareta W. Ardyani, National Crypto Institute, Bogor, Indonesia, +62 812 3832 5150

Infections caused by *C. albicans*

Generally, in immunocompromised individuals, *C. albicans* can cause bloodstream infections which are associated with high morbidity and mortality rates. It is reported in many literatures that mortality rates associated with systemic candidiasis are 30% higher than those associated with bacterial infections (see [7] for a review of this).

In many studies, it is reported that fungal infections are not uncommon in HIV disease. Oropharyngeal candidiasis is known to be the earliest indicator of HIV infection although other oral fungal diseases are also prevalent [5, 8]. It is reported that *Candida* species are among those essential microbial agents of severe periodontitis in HIV-infected patients (see [5] for a review of this).

In other reviews, it is revealed that *Candida* species accounted for 8% to 10% of all nosocomial bloodstream infections in the United States during 1990s, and *C. albicans* proves to be the most prevalent cause of candida blood stream infections.

It is widely known that *Candida* is the predominant cause of invasive fungal infections which account for 70% to 90% of all cases (see [9] for a review of this). Among all *Candida* species, *C. albicans* is reported to be by far the most common cause of candidiasis [9].

Candida species are also believed to be the main cause of device-related infections, particularly those which involve the blood stream and urinary tract. In fact, the medical consequences of device-related infections can be severe, including potentially life-threatening systemic infections and device malfunction that may require device removal, which is also often complicated by tissue destruction [6]. An implanted medical device with a detectable biofilm is often associated with these infections. In *C. albicans*, the biofilm formation happens through three developmental stages, including adherence of yeast cells to the device surface, formation of a matrix with dimorphic switching from yeast to hyphal forms, and increase in the matrix material taking on a three-dimensional architecture (see [6] for a review of this).

C. albicans morphogenesis

Candida albicans, along with many other fungal pathogens are able to grow as unicellular yeast cells or as filamentous hyphae, and can grow as either yeast or in hyphal forms in the host. Figure 1 shows the growth of *C. albicans* in yeast and hyphal forms.

Depending on the environmental conditions, *C. albicans* is capable of growing in either the yeast or the hyphal forms (which is why it is termed dimorphic). Under specific conditions, *C. albicans* cells grow as yeast, and under other

conditions, most cells grow as hyphae, and the switch from one pattern to another in response to external signals is rapid [10].

The switch between the yeast and hyphal growth patterns is reported to be a critical component of the ability of *C. albicans* to colonize as a commensal and for its virulence [7, 10, 11]. In the form of yeast cells, *C. albicans* is capable of outcompeting the faster growing bacterial flora and the immune response since they are small, non-adherent, and less immunogenic, and divide more rapidly than hyphal cells. On the other hand, in the form of hyphal cells, *C. albicans* can maintain itself on mucosal surfaces, and in immunocompromised individuals, enter the bloodstream, and cause infection [11].

In *C. albicans*, cellular morphogenesis is associated with changes in the composition and architecture of the cell wall. This will therefore influence detection by the host immune system and the subsequent response. Generally, the basic components of the *C. albicans* cell wall are similar in both yeast and hyphal forms, but the surface proteome and the amounts of individual pathogen-associated molecular patterns presented to immune cells differ substantially. Since the cell wall is highly regulated and responsive, it represents a moving target that serves as a significant challenge for the host immune system [12]. However, the interaction between the immune system and various morphogenetic forms of this fungus is not yet well understood.

The morphogenetic switch from yeast to hyphal cells is governed by various environmental signals, including pH, nutrient availability, temperature, and quorum sensing (see [7, 8, 11, 13] for reviews of this). Morphogenesis is believed to be one of the main factors making *C. albicans* an effective pathogen [13, 14, 15]. This study aims to investigate how morphogenesis is generated in *C. albicans* since it is vital for virulence and in what way it can be prevented. We are looking into mathematical models representing the mechanism of one of the signaling cascades regulating morphogenesis in *C. albicans*.

Signaling pathways for *C. albicans* morphogenesis

Several signaling cascades are responsible for morphogenesis in *C. albicans*. However, it is reported that the cAMP pathway is the most crucial, with most cues being regulated through the adenylyl cyclase, Cyr1p [7, 12, 15]. *C. albicans*, in its attempt to survive in the host's body, needs to adapt to the host environmental signals. Further, it also needs to adapt and respond to other microorganisms from the natural flora to set itself up within a niche. Microorganisms are also capable of communicating with themselves through quorum sensing (see [7, 15] for reviews of this). Quorum sensing is described as the regulation of genes in a density dependent manner and is established as contributing to pathogenicity of certain bacterial species through the regulation of essential virulence factors. It has been suggested that quorum sensing contributes to morphogenesis control in *C. albicans* [2].

Two distinct compounds are identified as quorum sensing molecules for *C. albicans*, namely farnesol which is generated by *C. albicans* itself, and 3-oxo-C12-homoserine lactone (HSL) which is secreted by the bacterium *Pseudomonas aeruginosa* (see [7, 14, 15, 16] for reviews of this). It is worth to note that 3-oxo-C12-homoserine lactone (HSL) does not enable *C. albicans* to communicate with itself but with other

bacteria. The two QSs (quorum sensing molecules) both act as inhibitors of the yeast-to-hyphal switch in *C. albicans* morphogenesis by downregulating the cAMP pathway [7, 12, 16]. The actual mechanism by which these QSs generate their effects on *C. albicans* is still currently unknown. Studies suggest that other pathways may also play a role in the quorum sensing process, or that the QSs are able to obstruct multiple processes which contribute to morphogenesis [2, 7, 17]. In this project, however, we focus on farnesol and its effects in blocking the cAMP pathway.

As mentioned earlier, the cAMP pathway is mainly regulated through the fungal adenylyl cyclase, Cyr1p. Several studies have reported that QSs obstruct filamentation by generating their effects on the essential components of the cAMP pathway, e.g. Cyr1p. It is likely that farnesol can bind to Cyr1p, forming a new complex Cyr1p~Farnesol which contributes to the inhibition of the cAMP pathway.

It has also been reported that Cyr1p is the major sensor of CO₂ [2]. Initially, CO₂ is needed for metabolism. It is converted into bicarbonate and when the amount of bicarbonate required for metabolism has been fulfilled, the increased concentrations of bicarbonate immediately activate Cyr1p, causing an increase in the intracellular concentration of cAMP and promoting filamentation (see [2, 15] for reviews of this). It is reported in Hall et al. (2010) that in low concentrations, CO₂ will be used for metabolism and when it exceeds the critical threshold, it promotes filamentation and subsequent surface invasion of *C. albicans*. Since Cyr1p is the major sensor of CO₂, it is likely that CO₂ can bind to Cyr1p, forming a new complex Cyr1p~CO₂ which increases cAMP concentrations.

In this study, we establish two models investigating the roles of farnesol and CO₂ in inhibiting and activating the cAMP pathway. The first model in which farnesol binds to Cyr1p, forming the complex Cyr1p~Farnesol which degrades cAMP molecules directly, suggests that under the parameter and initial values that we have chosen, morphogenesis can be prevented since the amount of cAMP molecules is considerably lower than its main inhibitor, the complex Cyr1p~Farnesol. On the other hand, the second model in which farnesol binds to Cyr1p, forming the complex Cyr1p~Farnesol which triggers the dissociation of the complex Cyr1p~CO₂ formed by the binding of Cyr1p and CO₂, indicates that morphogenesis is more likely to happen since the amount of Cyr1p~Farnesol falls at a very low level while the main agent of cAMP production, Cyr1p~CO₂, maintains a considerably higher concentration level.

II. MODEL DEVELOPMENT

Several studies have developed mathematical models investigating the regulation of signalling pathways in fungi. Leach et al. (2012) developed a mathematical model of the regulation of thermal adaptation in *Candida albicans* as heat shock response is essential for the virulence of this organism. As we mention earlier, morphogenesis is one of the main factors making *C. albicans* an effective pathogen and the cAMP pathway is believed to be the most crucial cascade governing it. Williamson et al. (2009) also developed mathematical models of the cAMP pathway, but in the fungus *Saccharomyces cerevisiae*. Since *C. albicans* is a major fungal pathogen and morphogenesis is one of the main factors

making this organism a pathogen, we are looking into modelling the cAMP pathway regulating it.

In this project, two different models are established to investigate the roles of farnesol and CO₂ in cAMP inhibition and production, and further, hyphal formation and morphogenesis. Since the exact mechanism of the QSMs in the cAMP pathway remains unknown, two possible scenarios are illustrated. As explained previously, farnesol affects morphogenesis by inhibiting the cAMP pathway in *C. albicans*. We assume that farnesol directly targets Cyr1p and both molecules bind together, forming the complex Cyr1p~Farnesol. The exact mechanism of how this complex works to inhibit the cAMP pathway remains unknown. The current data that we have does not give adequate information on whether the complex directly or indirectly reduces cAMP.

The complex could reduce cAMP directly (Figure 2), or indirectly, by targeting the complex formed by CO₂ and Cyr1p, namely Cyr1p~CO₂ (Figure 3). As previously explained, the complex Cyr1p~CO₂ triggers the production of cAMP which leads to morphogenesis. If Cyr1p~Farnesol targets Cyr1p~CO₂ it is likely that Cyr1p~Farnesol will trigger the dissociation of Cyr1p~CO₂, returning it back to be Cyr1p and CO₂.

A. Model 1: Farnesol directly degrades cAMP

Figure 2 illustrates the first possible scenario. We assume that the following events occur in this scheme:

- Farnesol and CO₂ both target Cyr1p, forming complexes Cyr1p~Farnesol and Cyr1p~CO₂ respectively
- Cyr1p itself can produce cAMP by changing ATP into cAMP. Since ATP is available in abundance in *C. albicans*, we do not include ATP as one of the variables in the model
- Both Cyr1p~Farnesol and Cyr1p~CO₂ complexes can dissociate and return to their original forms, which is why the associated reactions are reversible
- cAMP is produced by Cyr1p which changes ATP into cAMP, as well as the binding of Cyr1p~CO₂ and ATP, the second happening at much a higher rate than the first
- Cyr1p~Farnesol directly degrades cAMP at some rate g .

The events occurring in Figure 2 can be translated into the following set of equations (see Table 1 for definitions of the variables and Table 2 for the parameters):

$$\begin{aligned}\frac{dF}{dt} &= X - aFC + bC_f - \alpha F \\ \frac{dC}{dt} &= Y - aFC + bC_f - cC - dC_k + eC_k - \beta C \\ \frac{dK}{dt} &= Z - dCK + eC_k - \gamma K \\ \frac{dC_f}{dt} &= aFC - bC_f - gC_f cAMP - \delta C_f \\ \frac{dC_k}{dt} &= dCK - eC_k - fC_k - \eta C_k \\ \frac{dcAMP}{dt} &= cC + fC_k - gC_f cAMP - \zeta cAMP\end{aligned}$$

B. Model 2: Farnesol targets Cyr1p~CO₂

In Figure 3, the second possible scenario is illustrated. The mechanisms are similar to those in the first scenario, only that this time, the Cyr1p~Farnesol complex indirectly inhibits the

production of cAMP, by triggering the dissociation of the Cyr1p~CO₂ complex, leading it to return to its original forms. We assume that the complex Cyr1p~Farnesol gets used up in the system to dissociate the complex Cyr1p~CO₂, making it return to its original forms and therefore unable to produce cAMP. This scenario can be summarized in the following set of equations, with all the variables and parameters given in Tables 2 and 3.

$$\begin{aligned}\frac{dF}{dt} &= X - aFC + bC_f - \alpha F \\ \frac{dC}{dt} &= Y - aFC + bC_f - cC - dCK + eC_k + hC_f C_k - \beta C \\ \frac{dK}{dt} &= Z - dCK + eC_k + hC_f C_k - \gamma K \\ \frac{dC_f}{dt} &= aFC - bC_f - hC_f C_k - \delta C_f \\ \frac{dC_k}{dt} &= dCK - eC_k - fC_k - hC_f C_k - \eta C_k \\ \frac{dcAMP}{dt} &= cC + fC_k - \zeta cAMP\end{aligned}$$

C. Parameter Values

Since the currently available data does not provide adequate information about the mechanism by which farnesol and CO₂ generate their effects of inhibition and production of cAMP, we can only estimate the values of each parameter used in the models. The parameter values are chosen to be of a similar magnitude to the relevant parameters in literature [9]. We refer to this literature because this study investigates the same organism as we do. The parameter values used in this paper should be relevant to our model since they are taken from the same fungus. However, the binding rates used in [9] are unusually large. Therefore, to maintain biologically realistic behavior of our models, we change the binding rate values into those listed in Table 2.

For basal production of farnesol, Cyr1p, and CO₂ we choose large rates because we assume that *C. albicans* produces farnesol and Cyr1p in large amounts, while CO₂ is available abundantly in the environment. We put $c \ll 1$ (refer to Figure 2 and Figure 3) because we assume this occurs at a low basal rate in the absence of an activating trigger such as CO₂, which is why we also set $f \gg c$ since f is the production rate of cAMP by the complex Cyr1p~CO₂. The complete summary of the default parameter values and initial concentrations we use in this project is listed in Table 2 and Table 3 respectively.

III. RESULTS

Results and analysis of Model 1

Model 1 investigates the role of farnesol on inhibition of the cAMP pathway regulating morphogenesis in *C. albicans* by degrading cAMP directly. In Figure 4, we can observe how the system will behave in the absence of farnesol or CO₂. As explained previously, farnesol binds to Cyr1p and the two molecules form the complex Cyr1p~Farnesol which degrades cAMP, while CO₂ binds to Cyr1p, forming the complex Cyr1p~CO₂ which produces cAMP at a high rate. If farnesol does not exist, then we can expect that cAMP will be produced abundantly (see Figure 4A). On the contrary, if CO₂ does not exist, we can expect that cAMP, which is produced

only by Cyr1p, gets degraded very quickly by Cyr1p~Farnesol (see Figure 4B).

In Figure 4A, we can see that cAMP has a high concentration with the absence of farnesol. Even though CO₂ gets used up, but Cyr1p and Cyr1p~CO₂ maintain high concentrations, which enable them to produce more cAMP molecules. In Figure 4B, where there is no CO₂ in the system, we can observe that cAMP is degraded despite having a high initial concentration. Figure 4 outlines the effects of farnesol and CO₂ on cAMP inhibition and production more clearly since we can observe the behavior of cAMP under the influence of the associated molecules.

In Figure 5, we can observe the behavior of the system when both farnesol and CO₂ are present. Figures 5A and 5B share similar behaviors, despite the fact that we make g , the rate at which Cyr1p~Farnesol degrades cAMP, a lot bigger than the default value in Figure 5B. In both figures, we can observe that cAMP falls to a low concentration while Cyr1p~Farnesol maintains a considerably higher concentration, indicating that cAMP degradation will still continue.

In Figure 6, we vary the values of X and Z , the production rates of farnesol and CO₂ respectively. The default values of X and Z are already much larger than other parameters (see Table 2), making them the key parameters to the system. In Figure 6A, where we set X much larger than Z , we can observe that cAMP concentration is even lower than that in Figure 5. This shows that with a much larger production rate, farnesol can generate its effect in inhibiting the cAMP pathway more effectively by degrading more cAMP molecules. In Figure 6B, where we set Z much larger than X , we can observe that cAMP concentration is higher than that in Figure 5. Moreover, the concentration of Cyr1p~Farnesol keeps decreasing as there are more cAMP molecules to be degraded. The complex Cyr1p~CO₂ has a considerably higher concentration than Cyr1p~Farnesol, suggesting that more cAMP molecules will be produced within the system. With a much larger production rate of CO₂, it is likely that cAMP production will increase and therefore promote morphogenesis.

In Figure 7, we illustrate the relationships of X and Z with their associated molecules, farnesol and CO₂ respectively, and cAMP at steady state. Figure 7A shows the relationships of X with farnesol and cAMP. As X increases, the concentration of farnesol also increases since X is the key parameter determining farnesol concentration. On the contrary, as X increases, cAMP decreases, since more farnesol will be produced and therefore more cAMP will be degraded. In Figure 7B, we illustrate the relationships of Z with CO₂ and cAMP. As Z increases, the amount of CO₂ also increases and therefore, the amount of cAMP also increases since more CO₂ will form more Cyr1p~CO₂, the main agent of cAMP production.

In Figure 8, we vary more parameters to observe cAMP behaviour more closely at steady state. We set g , the rate at which Cyr1p~Farnesol degrades cAMP, much larger than the default value. In Figure 8A, we make g and X much bigger than the default values which automatically results in high concentrations of both farnesol and Cyr1p~Farnesol. We can observe that cAMP 'does not stand a chance', as shown in Figure 8A where cAMP gets degraded very quickly and approaches 0. Moreover, Figure 8A shows a sudden spike at

the amount of farnesol as X increases, but then farnesol increases smoothly after. This is because we also put g large, so more Cyr1p~Farnesol is needed, which is why more farnesol gets used up.

In Figure 8B, we increase g and reduce α , the binding rate of farnesol and Cyr1p. This setting gives an increase of cAMP concentration and a constant farnesol concentration at first, but then farnesol starts to increase as X increases, making cAMP decrease since more Cyr1p~Farnesol will be produced if farnesol increases and therefore more cAMP will be degraded. In Figure 8C, we illustrate the relationships of Z with CO₂ and cAMP. As Z increases, the amount of CO₂ also quickly increases. However, the amount of cAMP increases very slowly because g is still much larger than the default value. In Figure 8D, we set d , the binding rate of Cyr1p and CO₂, much smaller than the default value. Under this setting, as Z increases, CO₂ takes time to finally increase after staying constant. However, cAMP does not increase even though Z and CO₂ are increasing since g is still much larger than the default value.

Results and analysis of Model 2

Model 2 investigates the role of farnesol on inhibition of the cAMP pathway regulating morphogenesis in *C. albicans* by triggering the dissociation of the complex Cyr1p~CO₂ so it cannot produce cAMP at a high rate. Figure 9 shows how the system will behave in the absence of farnesol or CO₂. If farnesol does not exist in the system, there will be no Cyr1p~Farnesol produced, which means that there are no molecules triggering the dissociation of Cyr1p~CO₂. Hence, Cyr1p~CO₂ will continue producing cAMP at a high rate. In Figure 9A, we can observe that the cAMP concentration is already high, but the concentrations of Cyr1p~CO₂ and Cyr1p are even higher. Both Cyr1p~CO₂ and Cyr1p are cAMP production agents, which means that if they retain high concentrations, cAMP production will continue. This condition will promote morphogenesis. Figure 9B shows how the system will behave in the absence of CO₂, and therefore cAMP will be produced by Cyr1p alone. Despite having a high initial concentration, cAMP gradually decreases since it is only produced at a low rate by Cyr1p and naturally degraded.

Figure 10 shows how the system will behave in the presence of both farnesol and CO₂. We can observe similar behaviours in Figures 10A and 10B, only that in Figure 10A, Cyr1p~Farnesol lasts a bit longer in the system since in Figure 10B, we set h , the rate at which Cyr1p~Farnesol triggers the dissociation of Cyr1p~CO₂, much larger than the default value. In both Figures 10A and 10B, we can observe that cAMP has a higher concentration than farnesol and Cyr1p~Farnesol. Moreover, Cyr1p~CO₂ maintains the highest concentration, which means that the molecule can still produce cAMP and it is likely that cAMP concentration will increase, which therefore leads to morphogenesis. However, this does not mean that this mechanism fails to inhibit morphogenesis in *C. albicans* and that the mechanism in Model 1 performs better. Instead, since the cAMP concentrations in both Models 1 and 2 are similar (see Figures 5A, 5B, 10A, and 10B), this may suggest that farnesol performs its effects more effectively on the inhibition of the cAMP pathway in Model 2.

Figure 11 shows the behavior of the system when we vary the key parameters X and Z determining the amounts of farnesol and CO_2 respectively. In Figure 11A, we set X , the production rate of farnesol, much larger than its default value. Since X is big, we can observe that farnesol has a very high concentration, which means it will produce more Cyr1p~Farnesol. Cyr1p~Farnesol triggers the dissociation of Cyr1p~ CO_2 and gets used up quickly, but when Cyr1p~ CO_2 falls low, Cyr1p~Farnesol gradually increases. Since Cyr1p and Cyr1p~ CO_2 fall to very low concentrations, cAMP will also gradually decrease since its production agents are no longer present. On the other hand, in Figure 11B where we set Z , the production rate of CO_2 , much larger than its default value, we can observe that CO_2 has a very high concentration. Moreover, we can also observe that Cyr1p and Cyr1p~Farnesol get used up very quickly. We can see that cAMP already has a high concentration, but Cyr1p~ CO_2 has an even higher one, indicating that cAMP production will continue. Meanwhile, farnesol also has a high concentration, but with Cyr1p gone, it cannot produce Cyr1p~Farnesol which triggers the dissociation of Cyr1p~ CO_2 . Under this condition, morphogenesis is likely to happen.

In Figure 12, we illustrate the relationships of X and Z with their associated molecules, farnesol and CO_2 respectively, and cAMP, at steady state. Figure 12A shows the relationships of X with farnesol and cAMP. As X increases, the amount of farnesol also increases since X is the key parameter determining farnesol concentration. On the contrary, as X increases, cAMP decreases, since more farnesol will be produced and therefore more Cyr1p~Farnesol will be produced to trigger the dissociation of Cyr1p~ CO_2 so this complex cannot produce cAMP at a high rate. In Figure 12B, we illustrate the relationships of Z with CO_2 and cAMP. As Z increases, the amount of CO_2 also increases and therefore, the amount of cAMP should also increase since more CO_2 will form more Cyr1p~ CO_2 , the main agent of cAMP production. However, Figure 12B shows that as Z increases, cAMP slowly decreases. This indicates that the mechanism in Model 2, in which farnesol targets Cyr1p~ CO_2 by triggering its dissociation through Cyr1p~Farnesol, is more effective in inhibiting the cAMP pathway because even when Z and CO_2 increase, cAMP still decreases.

Figure 12B shows a peculiar relationship of Z with CO_2 and cAMP because cAMP is supposed to increase when Z and CO_2 increase. We run more simulations to investigate this case more deeply. In Figure 13, we illustrate the relationships of Z with CO_2 and cAMP, and of Z with Cyr1p~ CO_2 and cAMP, at steady state where we set h , the rate at which Cyr1p~Farnesol triggers the dissociation of Cyr1p~ CO_2 , equal to g , the rate at which Cyr1p~Farnesol degrades cAMP in Model 1. Under this new chosen value of h , we can observe that as Z increases, the amounts of CO_2 , Cyr1p~ CO_2 and cAMP also increase.

By using the default value of h , we run another simulation illustrating the relationships of Z with Cyr1p~Farnesol, Cyr1p~ CO_2 and cAMP at steady state. In Figure 14, we can observe that as Z increases, initially cAMP and Cyr1p~ CO_2 increase as well while Cyr1p~Farnesol stays low. However, when Cyr1p~Farnesol starts to increase as Z also increases, both cAMP and Cyr1p~ CO_2 start decreasing because

Cyr1p~Farnesol will promote the dissociation of Cyr1p~ CO_2 so this complex cannot produce cAMP at a high rate.

In Figure 15, we vary more parameters to observe cAMP behaviour more closely. We set h , the rate at which Cyr1p~Farnesol triggers the dissociation of Cyr1p~ CO_2 , much larger than the default value. In Figure 15A, we make h and X much bigger than the default values which automatically results in high concentrations of both farnesol and Cyr1p~Farnesol. We can observe that cAMP gets degraded very quickly. Moreover, Figure 15A shows that farnesol increases more rapidly as cAMP gets degraded completely.

In Figure 15B, we increase h and reduce a , the binding rate of farnesol and Cyr1p. This setting gives an increase of cAMP concentration and a constant farnesol concentration at first, but then farnesol starts to increase as X increases, making cAMP stay constant since more Cyr1p~Farnesol will be produced if farnesol increases and therefore more Cyr1p~ CO_2 will dissociate and cAMP cannot be produced at a high rate. In Figure 15C, we illustrate the relationships of Z with CO_2 and cAMP. As Z increases, the amount of CO_2 also quickly increases. However, the amount of cAMP increases very slowly because h is still much larger than the default value. In Figure 15D, we set d , the binding rate of Cyr1p and CO_2 , much smaller than the default value. Under this setting, as Z increases, CO_2 takes time to finally increase after staying constant. cAMP immediately increases, since d is very small so it is solely produced by Cyr1p and even though h is large, Cyr1p~Farnesol does not directly target cAMP molecules. However, when CO_2 finally increases, cAMP suddenly stays constant because at this point, more Cyr1p~ CO_2 will be produced and dissociate again since h is large.

IV. DISCUSSION

Many studies have reported that mortality rates associated with fungal infections are considerably higher than those associated with bacterial infections. *Candida* species are reported to be the predominant cause of invasive fungal infections. They are the main agents of candidiasis, a fungal infection widely known as thrush which usually affects the skin, gastrointestinal, vaginal and oral tracts, and blood. Among all *Candida* species, *Candida albicans* is reported to be the main cause of candidiasis.

Morphogenesis in *C. albicans* is reported to be one of the main factors playing a vital role in the species pathogenicity. There are several signaling cascades regulating the morphogenetic switch in *C. albicans* from yeast to hyphal cells. It is reported that the cAMP pathway is the most crucial, with most signals governed through the adenylyl cyclase, Cyr1p. In this study, we investigate the roles of a quorum sensing molecule, farnesol, in obstructing this pathway, and of CO_2 in activating it. Farnesol can bind to Cyr1p, forming a new complex Cyr1p~Farnesol, which plays a crucial part in blocking the cAMP pathway. Cyr1p can also produce cAMP by changing ATP molecules, which are available abundantly in the environment, into cAMP molecules. It can also bind to CO_2 and form a new complex Cyr1p~ CO_2 which is the main agent in cAMP production.

However, the exact mechanism at which farnesol generates its effect on the inhibition of the cAMP pathway is

currently unknown. We investigate two possible scenarios, one where farnesol directly degrades cAMP (see Figure 2) and another where farnesol triggers the dissociation of Cyr1p~CO₂ which is the main agent of cAMP production through the complex Cyr1p~Farnesol (see Figure 3).

In Model 1, where farnesol binds to Cyr1p to form Cyr1p~Farnesol and this complex generates its effect in downregulating the cAMP pathway by directly degrading cAMP molecules, we observe similar trends happening in the simulations that we run (see Figure 5). Cyr1p~Farnesol will maintain the highest concentration of all molecules in the system when all variables are present, indicating that under the default parameter values and the chosen initial concentrations, the cAMP pathway is successfully downregulated and therefore morphogenesis can be inhibited. Even though the complex Cyr1p~CO₂ also has considerably high concentration, meaning that it can produce more cAMP molecules at a high rate, the cAMP concentration in the system falls low since cAMP will be degraded by Cyr1p~Farnesol.

In Model 2, where farnesol also binds to Cyr1p to form Cyr1p~Farnesol and this complex generates its effect in blocking the cAMP pathway by triggering the dissociation of the complex Cyr1p~CO₂ to return to its original forms so it cannot produce cAMP at a high rate, we observe different behavior of the system from that that we have in the simulations of Model 1. In Model 1, we have Cyr1p~Farnesol retaining the highest concentration, indicating that morphogenesis is inhibited. However, in the simulations that we run for Model 2, the complex Cyr1p~Farnesol falls to a very low level. This does not mean that the system fails to inhibit morphogenesis since the concentrations of cAMP in the simulations of both models are similar.

We can observe the behavior of both models more closely in Figures 7 and 12. Figures 7A and 12A share similar behavior when we illustrate the relationships of X with farnesol and cAMP. Since X is the key parameter determining farnesol concentration, we can observe that as X increases, farnesol also increases. If farnesol increases, then it only makes sense if Cyr1p~Farnesol increases and therefore, cAMP will decrease, either degraded by Cyr1p~Farnesol directly or produced in a much lower rate since Cyr1p~CO₂ dissociates at a high rate. Figure 7B shows an expected behavior since Z , CO₂ and cAMP are directly linked to each other. With Z being the key parameter determining CO₂ concentration, it is obvious if Z increases, then CO₂ also increases. CO₂ binds to Cyr1p, producing Cyr1p~CO₂ which produces cAMP at a high rate. As CO₂ increases, cAMP also increases. However, Figure 12B shows a surprising behavior since as Z and CO₂ increase, cAMP decreases. This peculiar behaviour is likely due to fact that h , the rate at which Cyr1p~Farnesol triggers the dissociation of Cyr1p~CO₂, is considerably larger than g , the rate at which Cyr1p~Farnesol degrades cAMP directly in Model 1, so Cyr1p~Farnesol generates its role more effectively. Under the default value of h , we can observe that the role of farnesol in inhibiting the cAMP pathway is really strong that cAMP will still decrease even when Z and CO₂ increase. When we run the simulations where $h = g$, we observe similar relationships of Z with CO₂ and cAMP in both models, i.e. when Z increases, CO₂ and cAMP also increase. The key point which makes Model 2 appears to perform a more effective mechanism in inhibiting

the cAMP pathway is the chosen value of h which is much larger than that of g . When $h = g$, it is likely that both models are equally effective in inhibiting the cAMP pathway.

The actual biological mechanism which happens in the system is not yet well understood. Both scenarios we predict in this study, where farnesol directly degrades cAMP through the complex Cyr1p~Farnesol and where farnesol triggers the dissociation of Cyr1p~CO₂ so this complex cannot produce cAMP at a high rate, are possible. Our models suggest that under the default parameter values and initial concentrations, morphogenesis can be inhibited since the concentration of cAMP within the system is low. Further, we observe that Model 2 demonstrates a more effective mechanism in inhibiting the cAMP pathway since under the default parameter values and the chosen initial concentrations, cAMP will keep decreasing even when Z and CO₂ increase.

It is also possible that both scenarios happen simultaneously, that they are not two separate mechanisms. Since we currently do not know how farnesol actually generates its effect in obstructing the cAMP pathway, it is possible that the complex Cyr1p~Farnesol degrades cAMP directly and triggers the dissociation of the complex Cyr1p~CO₂ at the same time. If this is what happens, the mechanism can be illustrated in Figure 16.

The mechanism illustrated in Figure 16 can be translated to the following set of equations (see Table 1 for the definition of the variables and Table 2 for parameters).

$$\begin{aligned} \frac{dF}{dt} &= X - aFC + bC_f - aF \\ \frac{dC}{dt} &= Y - aFC + bC_f - cC - dCK + eC_k + hC_fC_k - \beta C \\ \frac{dK}{dt} &= Z - dCK + eC_k + hC_fC_k - \gamma K \\ \frac{dC_f}{dt} &= aFC - bC_f - gC_f cAMP - hC_fC_k - \delta C_f \\ \frac{dC_k}{dt} &= dCK - eC_k - fC_k - hC_fC_k - \eta C_k \\ \frac{dcAMP}{dt} &= cC + fC_k - gC_f cAMP - \zeta cAMP \end{aligned}$$

If the mechanism illustrated in Figure 16 is what really happens biologically, it is worth investigating the behavior of the system numerically. Since farnesol will play a bigger role (to degrade cAMP directly and promote dissociation of Cyr1p~CO₂), it only makes sense if the system will need more farnesol to run if farnesol is lost in both of these reactions. Under the parameter and initial values that we have chosen previously, it is likely that morphogenesis will still happen because farnesol will run out very quickly and therefore cAMP molecules produced will remain high within the system. However, if the system is given a decent amount of farnesol, then under this mechanism morphogenesis can be inhibited since the amount of cAMP molecules will be low.

V. CONCLUSIONS

The main purpose of this study is to investigate the roles of farnesol and CO₂ in cAMP inhibition and production, and further, hyphal formation and morphogenesis. Farnesol, being a quorum sensing molecule downregulating the cAMP pathway, is known to play a vital role in cAMP inhibition. This fact has been documented in many biology papers [1, 2,

3, 8, 14, 23]. However, the actual mechanism of how farnesol generates its effect in cAMP inhibition is currently unknown. In this study, we present two possible scenarios in which farnesol generates its effect in downregulating the cAMP pathway and CO₂ in activating it.

Both models that we present suggest that under the default parameter values and initial concentrations, cAMP concentration falls low. Throughout our analysis, we have highlighted that Model 2 indicates a more effective mechanism in inhibiting the cAMP pathway since cAMP concentration keeps decreasing even when Z, the production rate of CO₂, and CO₂ increase despite the fact that CO₂ is vital for cAMP production. This shows that under the default parameter values and initial concentrations, the inhibition of the cAMP pathway is more successful in Model 2 compared to that in Model 1, since in Model 1, we have presented that as Z and CO₂ increase, cAMP also increases.

The cAMP pathway is reported to be the most crucial cascade regulating hyphal formation and morphogenesis in *C. albicans* which are vital for its virulence. Through this study, we have presented that Model 2 develops a more effective mechanism in downregulating the cAMP pathway under the default parameter values and initial concentrations. Therefore, if we could design a therapeutic molecule to treat fungal infections caused by *C. albicans*, the molecule should target Cyr1p~CO₂, the complex which produces cAMP at a high rate, instead of cAMP itself. Designing a molecule which degrades cAMP directly is not bad either, but as CO₂ in the environment increases, cAMP will still increase no matter how much degrading molecules are produced. Hence, designing a molecule which triggers the dissociation of the main agent of cAMP production, Cyr1p~CO₂, would be a better approach since cAMP will keep decreasing even when CO₂ in the environment increases.

ACKNOWLEDGMENT

We would like to thank Sara Jabbari and Rebecca Hall for their contribution in this work. Rebecca's extensive works on *Candida albicans* have helped shed light on the estimated system simulated in this project, and Sara's skills in mathematical modelling have been a really great help in analyzing the systems proposed in this work.

REFERENCES

- [1] Berman, Judith. 2012. *Candida albicans*. Current Biology. Vol. 22. R520
- [2] Hall, R.A., Cottier, F., Mühlshchegel, F.A. 2009. Molecular Networks in the Fungal Pathogen *Candida albicans*. Advances in Applied Microbiology. Vol. 67. pp. 191-212
- [3] Whiteway, M.. 2000. Transcriptional Control of Cell Type and Morphogenesis in *Candida albicans*. Current Opinion in Microbiology. Vol. 3. pp. 582-588
- [4] Hall, R.A., Mühlshchegel, F.A. 2010. A Multi-Protein Complex Controls cAMP Signalling and Filamentation in the Fungal Pathogen *Candida albicans*. Molecular Biology. Vol. 75. pp. 534-537
- [5] McAlester, G., O'Gara, F., Morrissey, J.P. 2008. Signal-mediated Interactions between *Pseudomonas aeruginosa* and *Candida albicans*. Journal of Medical Microbiology. Vol. 57. pp. 563-569
- [6] Ramage, G., Saville, S.P., Wickes, B.L., Lopez-Ribot, J.L. 2002. Inhibition of *Candida albicans* Biofilm Formation by Farnesol, a Quorum-Sensing Molecule. Applied and Environmental Microbiology. Vol. 68. pp. 5459-5463
- [7] Hall, R.A., Turner, K.J., Chaloupka, J., Cottier, F., De Sordi, L., Sanglard, D., Levin, L.R., Buck, J., Mühlshchegel, F.A. 2011. The Quorum-Sensing Molecules Farnesol/Homoserine Lactone and Dodecanol Operate via Distinct Modes of Action in *Candida albicans*.

- Eukaryotic Cell. Vol. 10. pp. 1034-1042
- [8] Hall, R.A. 2015. Dressed to Impress: Impact of Environmental Adaptation on the *Candida albicans* Cell Wall. Molecular Biology. Vol. 97. pp. 7-17
- [9] Kojic, E.M., Darouiche, R.O. 2004. *Candida* Infections on medical Devices. Clinical Microbiology Reviews. Vol. 17. pp. 255-267
- [10] Whiteway, M., Bachewich, C. 2007. Morphogenesis in *Candida albicans*. Annu Rev Microbiol. Vol. 61. pp. 529-553
- [11] Almirante, B., Rodriguez, D., Park, B.J., Cuenca-Estrella, M., Planes, A.M., Almela, M., Mensa, J., Sanchez, F., Ayats, J., Gimenez, M., Saballs, P., Fridkin, S.K., Morgan, J., Rodriguez-Tudela, J.L., Warnock, D.W., Pahissa, A., The Barcelona Candidemia Project Study Group. 2005. Epidemiology and Predictors of Mortality in Cases of *Candida* Bloodstream Infection: Results from Population-Based Surveillance, Barcelona, Spain, from 2002 to 2003. Journal of Clinical Microbiology. Vol. 43. pp. 1829-1835
- [12] Gow, N.A.R., van de Veerdonk, F.L., Brown, A.J.P., Netea, M.G. 2013. *Candida albicans* Morphogenesis and Host Defence: Discriminating Invasion from Colonisation. Nat Rev Microbiol. Vol 10. pp. 112-122
- [13] Brown, A.J.P., Gow, N.A.R. 1999. Regulator Networks Controlling *Candida albicans* Morphogenesis. Trends in Microbiology. Vol. 7. No. 8
- [14] Kruppa, M. 2008. Quorum Sensing and *Candida albicans*. Mycoses. Vol. 52. pp. 1-10
- [15] Hall, R.A., De Sordi, L., MacCallum, D.M., Topal, H., Eaton, R., Bloor, J.W., Robinson, G.K., Levin, L.R., Buck, J., Wang, Y., Gow, N.A.R., Steegborn, C., Mühlshchegel, F.A. 2010. CO₂ Acts as A Signaling Molecule in Populations of the Fungal Pathogen *Candida albicans*. www.plosone.org. Vol. 6
- [16] Davis-Hanna, A. Piispanen, A.E., Stateva, L.I., Hogan, D.A. 2008. Farnesol and Dodecanol Effects on the *Candida albicans* Ras1-cAMP Signaling Pathway and the Regulation of Morphogenesis. Molecular Biology. Vol. 67. pp. 47-62
- [17] Hogan, D.A. 2006. Talking to Themselves: Autoregulation and Quorum Sensing in Fungi. Eukaryotic Cell. Vol. 5. pp. 613-619
- [18] Leach, M.D., Tyc, K.M., Brown, A.J.P., Klipp, E. 2012. Modelling the Regulation of Thermal Adaptation in *Candida albicans*, a Major Fungal Pathogen of Humans. PLOS ONE. Vol. 7. e32467
- [19] Biswas, S., van Dijck, P., Datta, A. 2007. Environmental Sensing and Signal Transduction Pathways Regulating Morphopathogenic Determinants of *Candida albicans*. Microbiology and Molecular Biology Reviews. Vol. 71. pp. 348-376
- [20] Shapiro, R.S., Cowen, L.E. 2012. Uncovering Cellular Circuitry Controlling Temperature-Dependent Fungal Morphogenesis. Virulence. Vol. 3. pp. 400-404
- [21] Cottier, F., Mühlshchegel, F.A. 2009. Sensing the Environment: Response of *Candida albicans* to the X Factor. FEMS Microbiol Lett. Vol. 295. pp. 1-9
- [22] Zacchi, L.F., Gomez-Raja, J., Davis, D.A. 2010. Msd3 Regulates Morphogenesis in *Candida albicans* through the TOR Pathway. Molecular and Cellular Biology. Vol. 30. pp. 3695-3710
- [23] Leroy, O., Gangneux, J., Montravers, P., Mira, J., Gouin, F., Sollet, J., Carlet, J., Reynes, J., Rosenheim, M., Regnier, B., Lortholary, O. 2009. Epidemiology, Management, and Risk Factors for Death of Invasive *Candida* Infections in Critical Care: A Multicenter, Prospective, Observational Study in France (2005-2006). Crit Care Med. Vol. 37. pp. 1612-1618
- [24] Samaranyake, L.P., Fidel, P.L., Naglik, J.R., Sweet, S.P., Teanpaisan, R., Cogan, M.M., Blignaut, E., Wanzala, P. 2002. Fungal Infections Associated with HIV Infection. Oral Diseases. Vol. 8 (Suppl. 2). pp. 151-160
- [25] Hogan, D.A., Vik, A., Kolter, R. 2004. A *Pseudomonas aeruginosa* Quorum-Sensing Molecule Influences *Candida albicans* Morphology. Molecular Biology. Vol. 54. pp. 1212-1223R. J. Vidmar. (1992, August). On the use of atmospheric plasmas as electromagnetic reflectors. *IEEE Trans. Plasma Sci.* [Online]. 21(3). pp. 876-880. Available: <http://www.halcyon.com/pub/journals/21ps03-vidmar>

Mareta W. Ardyani Mareta obtained her MSc in 2015 from the University of Birmingham, majoring in Mathematical Modelling in Biology. In accordance with her degree, she was (and still is) very interested in mathematical biology. Her project with Dr Sara Jabbari (School of Mathematics, University of Birmingham) and Dr Rebecca Hall (School of Biosciences, University of Birmingham) inspired her to do further works in the field of mathematical biology. After being employed by the Indonesian

Modelling the Effects of Farnesol and CO₂ on the cAMP Pathway Regulating Morphogenesis in *Candida albicans*

Ministry of National Development Planning in 2016, however, Mareta had to postpone any works related to her research on mathematical biology.

In the Ministry of National Development Planning, she worked under the Senior Advisor to the Minister on Institutional Affairs, providing academic and scientific recommendations regarding the cost and benefit analysis on various economically critical laws and regulations, resulting in the revocation of more than three hundreds regulations (both at national or regional levels) which are deemed problematic and allegedly scathe the progressive economic development that the President was working on.

After working for two years in the Ministry of National Development Planning, Mareta decided to retrace her steps in a more academic path, and subsequently made it to be one of the teaching staffs at one of the best

state-owned colleges in Indonesia, the National Crypto Agency. The college is operated under the wings of Indonesia's leading cyber security agency, the National Cyber and Crypto Agency. Teaching at a college heavily influenced by semi-military culture brought another challenging point of view in Mareta's professional growth. Having invested most of her time at university dealing with mathematical modelling in biology, she decided to challenge herself to a more complicated branch of mathematics and computer science, the art of cryptography and cryptanalysis. Though she is currently fighting her way to establish a relatively current field of mathematics, which she named the mathematical modelling in cryptography and cryptanalysis, she never lost her origin as a mathematical biologist, and hence continued to thrive in the research and works of mathematical modelling in biology.

Table 1: Definition of variables used in models

Variable	Definition
F	Farnesol
C	Cyr1p
K	CO ₂
C_f	Cyr1p~Farnesol
C_k	Cyr1p~ CO ₂
$cAMP$	cAMP

Table 2: Default parameter values used in the models. Note that some parameters are slightly adjusted from the estimations given in [18] to maintain biologically realistic behavior by the models.

Parameter	Description	Unit	Value	Source
X	Production rate of farnesol	nM sec ⁻¹	2×10^4	Estimation
Y	Production rate of Cyr1p	nM sec ⁻¹	3×10^4	Estimation
Z	Production rate of CO ₂	nM sec ⁻¹	2×10^4	Estimation
a	Binding rate of Cyr1p and farnesol	nM ⁻¹ sec ⁻¹	1.1×10^4	Estimation
b	Dissociation rate of Cyr1p~Farnesol	sec ⁻¹	2×10^{-2}	[18]
c	Production rate of cAMP from Cyr1p and ATP	sec ⁻¹	1×10^{-3}	Estimation
d	Binding rate of Cyr1p and CO ₂	nM ⁻¹ sec ⁻¹	1×10^4	Estimation
e	Dissociation rate of Cyr1p~ CO ₂	sec ⁻¹	3×10^{-2}	[18]
f	Production rate of cAMP from Cyr1p~ CO ₂	sec ⁻¹	1.2	Estimation
g	The rate at which Cyr1p~Farnesol degrades cAMP	nM ⁻¹ sec ⁻¹	1×10^{-10}	[18]
h	The rate at which Cyr1p~Farnesol triggers the dissociation of Cyr1p~ CO ₂	nM ⁻¹ sec ⁻¹	1.5×10^{-1}	Estimation
α	Natural degradation rate of farnesol	sec ⁻¹	2.4	[18]
β	Natural degradation rate of Cyr1p	sec ⁻¹	1.7	[18]
γ	Natural degradation rate of CO ₂	sec ⁻¹	2.35	[18]
δ	Natural degradation rate of Cyr1p~Farnesol	sec ⁻¹	2.26	[18]
η	Natural degradation rate of Cyr1p~ CO ₂	sec ⁻¹	2	[18]
ζ	Natural degradation rate of cAMP	sec ⁻¹	1.97	[18]

Table 3: Default initial concentration of variables.

Variable	Definition
Farnesol	$F(0) = 20000$
Cyr1p	$C(0) = 40000$
CO ₂	$K(0) = 20000$
Cyr1p~Farnesol	$C_f(0) = 0$
Cyr1p~ CO ₂	$C_k(0) = 0$
cAMP	$cAMP(0) = 0$

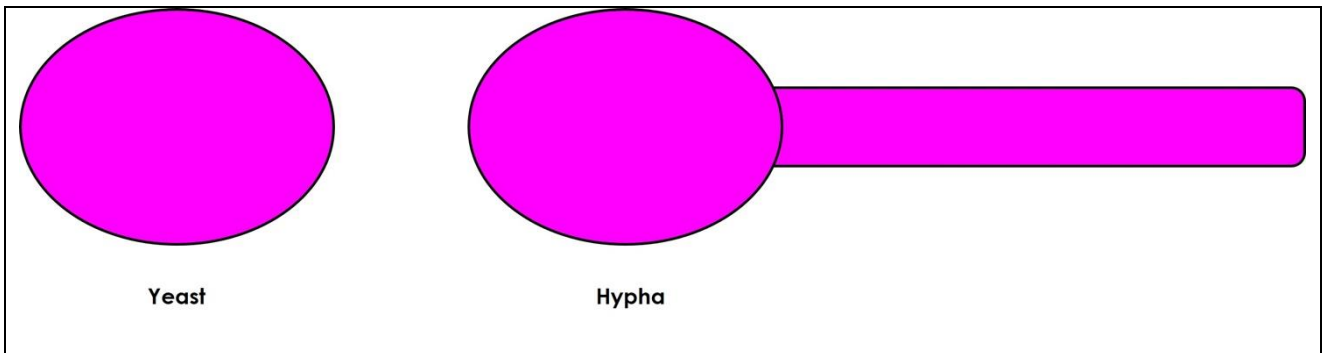


Figure 1: *C. albicans* can grow as yeast or hyphae

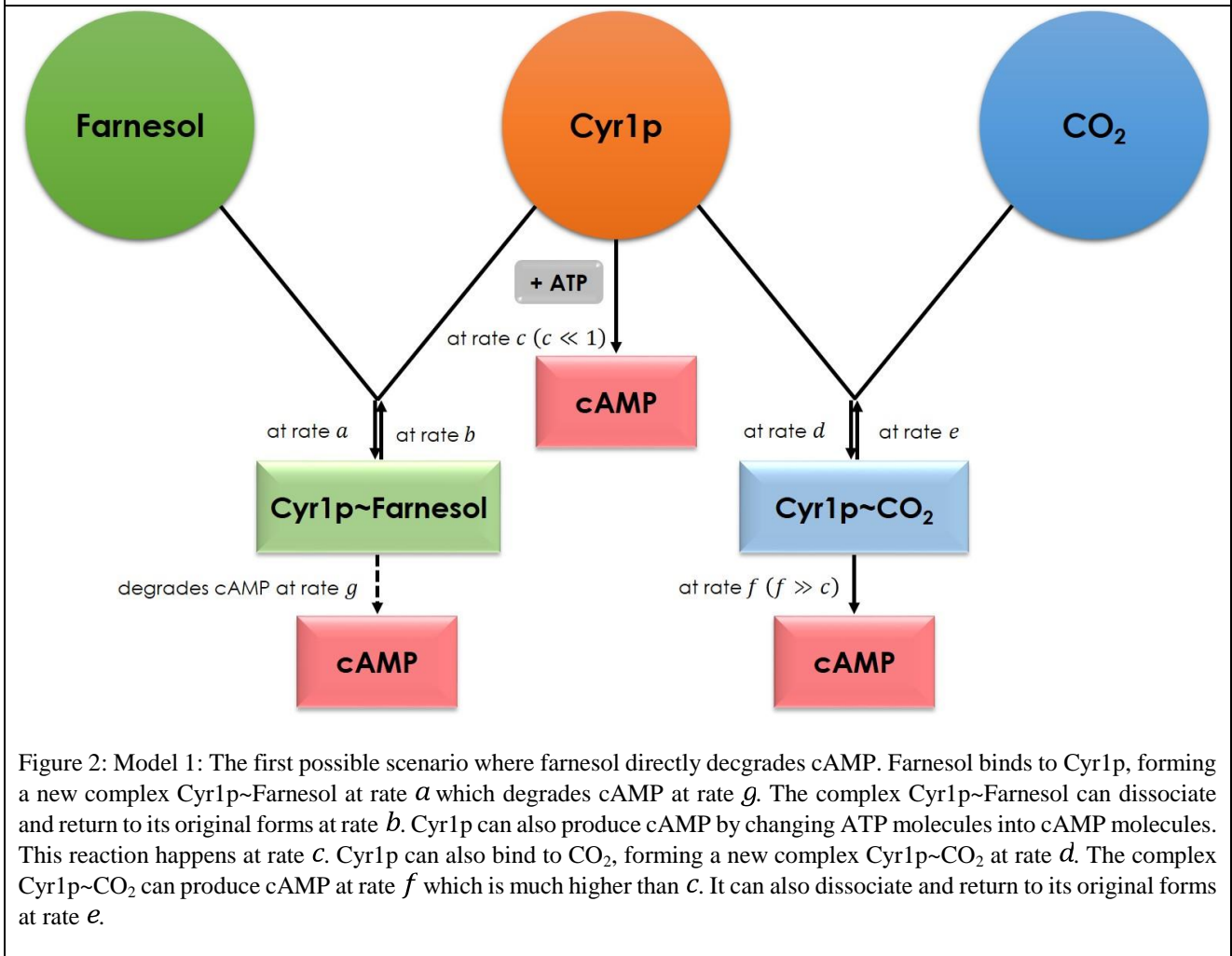


Figure 2: Model 1: The first possible scenario where farnesol directly degrades cAMP. Farnesol binds to Cyr1p, forming a new complex Cyr1p~Farnesol at rate a which degrades cAMP at rate g . The complex Cyr1p~Farnesol can dissociate and return to its original forms at rate b . Cyr1p can also produce cAMP by changing ATP molecules into cAMP molecules. This reaction happens at rate c . Cyr1p can also bind to CO₂, forming a new complex Cyr1p~CO₂ at rate d . The complex Cyr1p~CO₂ can produce cAMP at rate f which is much higher than c . It can also dissociate and return to its original forms at rate e .

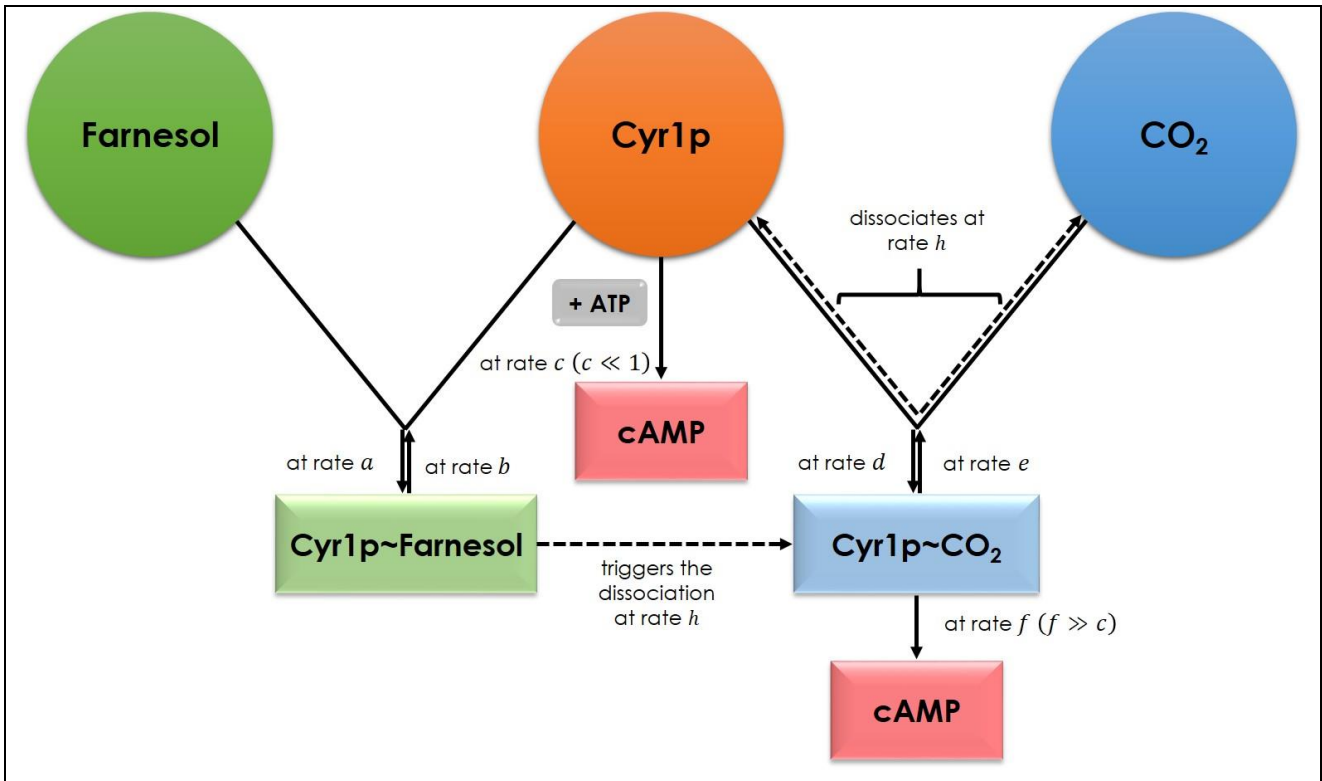
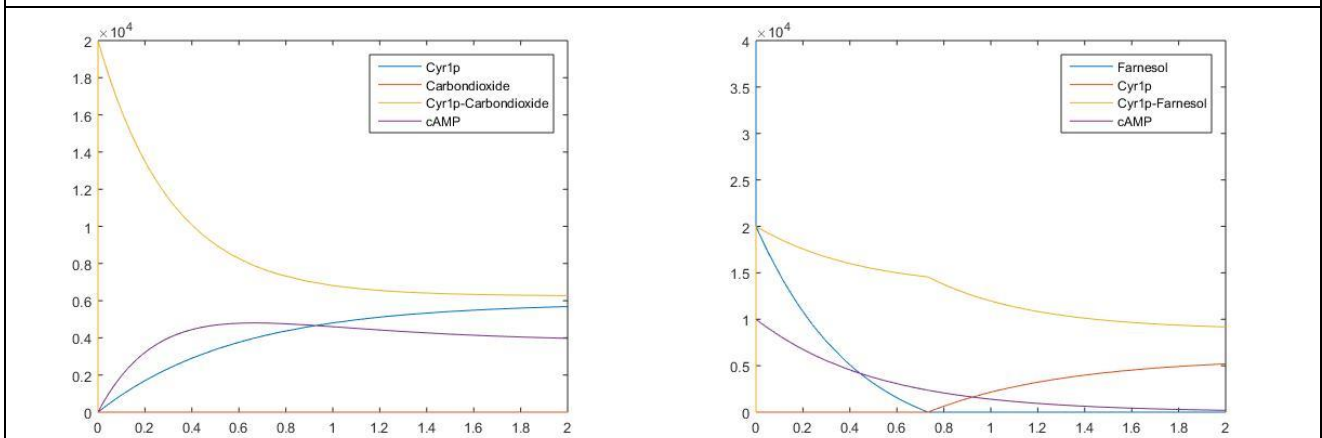


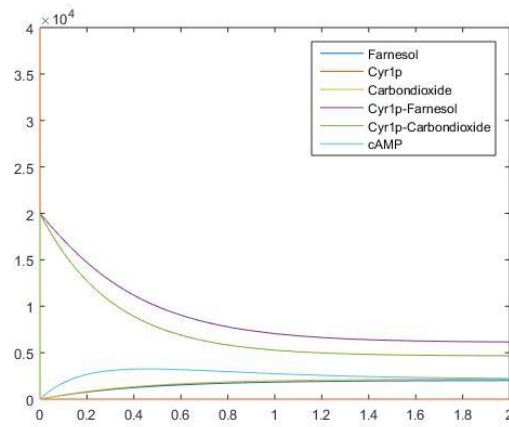
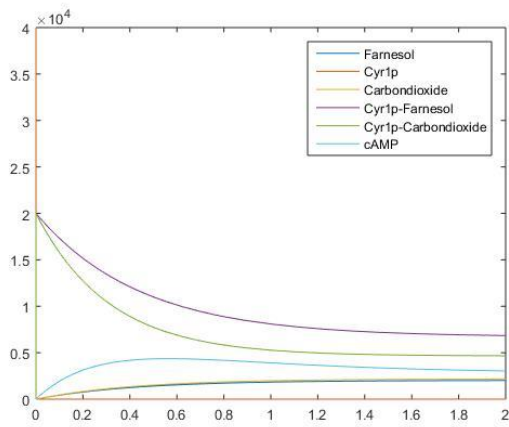
Figure 3: Model 2: The second possible scenario where farnesol targets Cyr1p~CO₂. Farnesol binds to Cyr1p, forming a new complex Cyr1p~Farnesol at rate *a* which triggers the dissociation of the complex Cyr1p~CO₂ at rate *h*. The complex Cyr1p~Farnesol can dissociate and return to its original forms at rate *b*. Cyr1p can also produce cAMP by changing ATP molecules into cAMP molecules. This reaction happens at rate *c*. Cyr1p can also bind to CO₂, forming a new complex Cyr1p~CO₂ at rate *d*. The complex Cyr1p~CO₂ can produce cAMP at rate *f* which is much higher than *c*. It can also dissociate and return to its original forms at rate *e*.



A. The simulation of Model 1 where farnesol does not exist in the system. The chosen initial concentrations are $C(0) = K(0) = 20000$ with $F(0) = 0, X(0) = 0$, and other default parameter values listed in Table 2.

B. The simulation of Model 1 where CO₂ does not exist in the system. The chosen initial concentrations are $F(0) = 40000$ and $cAMP(0) = 10000$ with $K(0) = 0, Z(0) = 0$, and other default parameter values listed in Table 2.

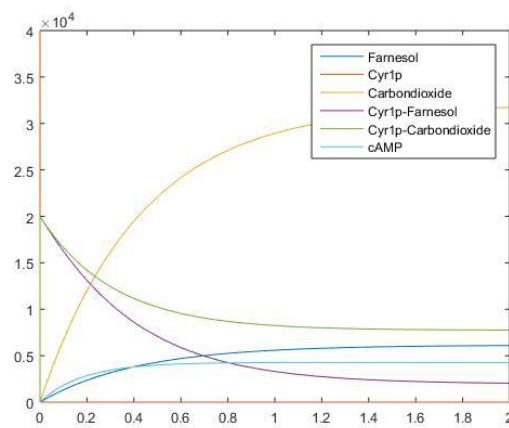
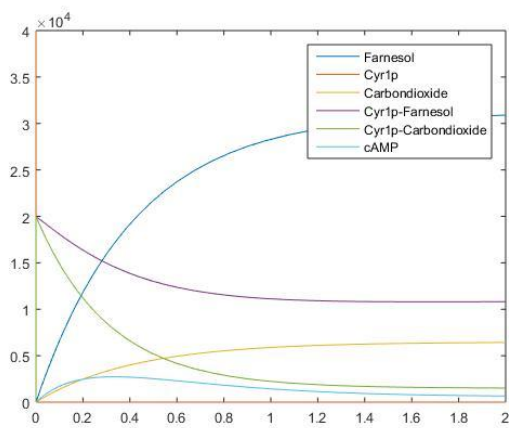
Figure 4: In these simulations, we investigate the behavior of the system where farnesol does not exist (Figure 4A) and where CO₂ does not exist (Figure 4B). When farnesol does not exist in the system, cAMP is produced by both Cyr1p at a low rate and Cyr1p~CO₂ at a high rate. Therefore, the amount of cAMP will be abundant within the system. On the contrary, when CO₂ does not exist in the system, cAMP is only produced by Cyr1p at a low rate. Therefore, it is degraded very quickly by Cyr1p~Farnesol.



A. The simulation of Model 1 where all molecules are present. The chosen initial values are $F(0) = K(0) = 20000$ and $C(0) = 40000$ with the default parameter values listed in Table 2.

B. The simulation of Model 1 where all molecules are present. The chosen initial values are $F(0) = K(0) = 20000$ and $C(0) = 40000$ with $g = 10^{-4}$ other default parameter values listed in Table 2.

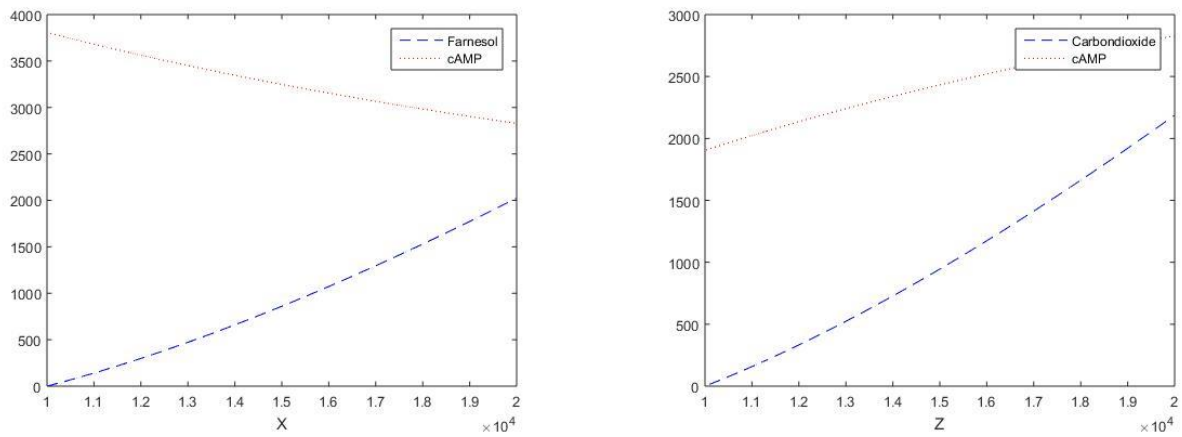
Figure 5: The simulations of Model 1 where all molecules are present in the system. The two simulations share similar trends despite g being much larger in Figure 5B. We can observe that, in both simulations, cAMP falls to a low concentration while Cyr1p-Farnesol maintains a considerably higher concentration, indicating that cAMP degradation will still continue.



A. The simulation of Model 1 where all molecules are present. The chosen initial values are $F(0) = K(0) = 20000$ and $C(0) = 40000$ with $X = 10^5$, $g = 10^{-4}$ and other default parameter values listed in Table 2.

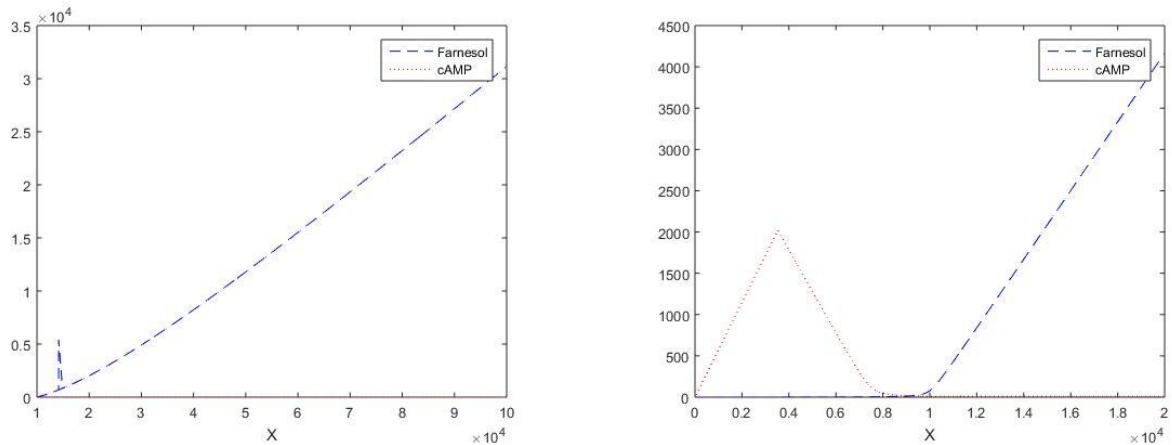
B. The simulation of Model 1 where all molecules are present. The chosen initial values are $F(0) = K(0) = 20000$ and $C(0) = 40000$ with $Z = 10^5$, $g = 10^{-4}$ and other default parameter values listed in Table 2.

Figure 6: In Figure 6A, where we set X much larger than Z , we can observe that cAMP concentration is even lower than that in Figure 5. This shows that with a much larger production rate, farnesol can generate its effect in inhibiting the cAMP pathway more effectively by degrading more cAMP molecules. In Figure 6B, where we set Z much larger than X , we can observe that cAMP concentration is higher than that in Figure 5. Moreover, the concentration of Cyr1p-Farnesol keeps decreasing as there are more cAMP molecules to be degraded. The complex Cyr1p- CO_2 has a considerably higher concentration than Cyr1p-Farnesol, suggesting that more cAMP molecules will be produced within the system.

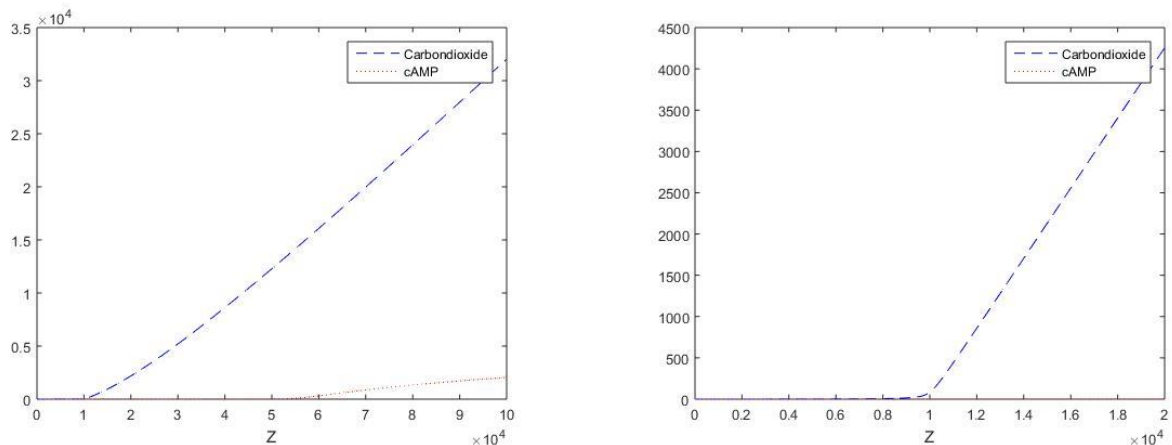


A. The relationship of X with farnesol and cAMP at steady state under default parameter values. B. The relationship of Z with CO₂ and cAMP at steady state under default parameter values.

Figure 7: In Figure 7A, we can observe that as X increases, the concentration of farnesol also increases. On the contrary, as X increases, cAMP decreases, since more farnesol will be produced and therefore more cAMP will be degraded. In Figure 7B, we can observe that as Z increases, the amount of CO₂ also increases and therefore, the amount of cAMP also increases since more CO₂ will form more Cyr1p~CO₂, the main agent of cAMP production.



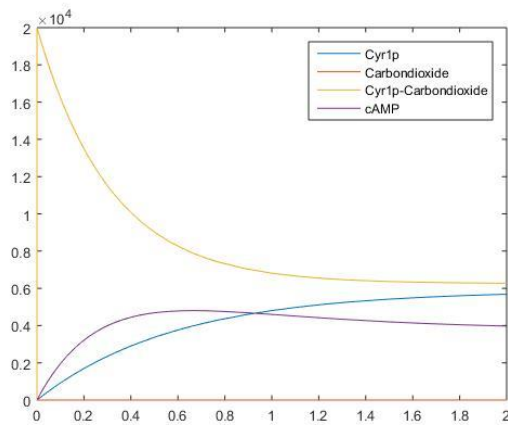
A. The relationship of X with farnesol and cAMP when $g = 6 \times 10^{-1}$ and $X = 10^5$ at steady state. B. The relationship of X with farnesol and cAMP when $g = 6 \times 10^{-1}$ and $a = 1.1$ at steady state.



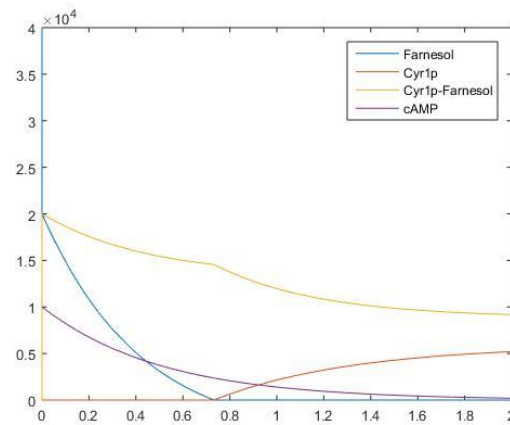
C. The relationship of Z with CO₂ and cAMP when $g = 6 \times 10^{-1}$ and $Z = 10^5$ at steady state. D. The relationship of Z with CO₂ and cAMP when $g = 6 \times 10^{-1}$ and $d = 1$ at steady state.

Figure 8: In Figure 8A, we make g and X much bigger than the default values which automatically result in high concentrations of both farnesol and Cyr1p~Farnesol, and therefore cAMP gets degraded very quickly and approaches 0. In Figure 8B, we increase g and reduce a , the binding rate of farnesol and Cyr1p. This setting gives an increase of cAMP concentration and a constant farnesol concentration at first, but then farnesol starts to increase as X increases, making cAMP decrease since more Cyr1p~Farnesol will be produced if farnesol increases and therefore more cAMP will be degraded. In Figure 8C, we illustrate the relationships of Z with CO₂ and cAMP. As Z increases, the amount of CO₂ also quickly increases. However, the amount of cAMP increases very slowly because g is still much larger than the default

value. In Figure 8D, we set d , the binding rate of Cyr1p and CO₂, much smaller than the default value. Under this setting, as Z increases, CO₂ takes time to finally increase after staying constant. However, cAMP does not increase even though Z and CO₂ are increasing since g is still much larger than the default value.

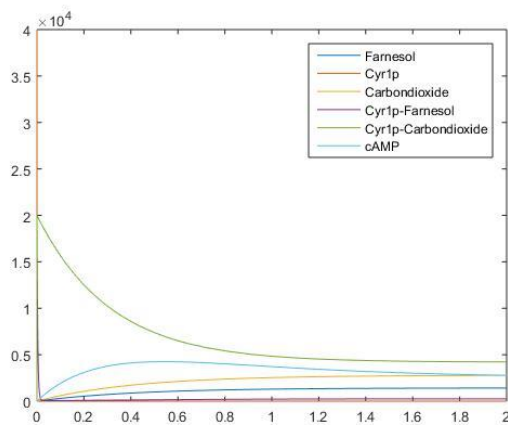


A. The simulation of Model 2 where farnesol does not exist in the system. The chosen initial concentrations are $C(0) = K(0) = 20000$ with default parameter values listed in Table 2.

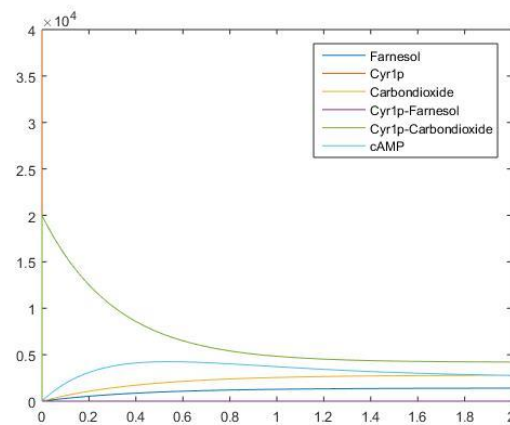


B. The simulation of Model 2 where CO₂ does not exist in the system. The chosen initial concentrations are $F(0) = 40000, K(0) = 20000$ and $cAMP(0) = 10000$ with default parameter values listed in Table 2.

Figure 9: In these simulations, we investigate the behavior of the system where farnesol does not exist (Figure 9A) and where CO₂ does not exist (Figure 9B). If farnesol does not exist in the system, there will be no Cyr1p~Farnesol produced, which means that there are no molecules triggering the dissociation of Cyr1p~CO₂. Hence, Cyr1p~CO₂ will continue producing cAMP at a high rate. In Figure 9A, we can observe that cAMP concentration is already high, but the concentrations of Cyr1p~CO₂ are even higher. Both Cyr1p~CO₂ and Cyr1p are cAMP production agents, which means that if they retain high concentrations, cAMP production will continue. Figure 9B shows how the system will behave in the absence of CO₂, and therefore cAMP will be produced by Cyr1p alone. Despite having a high initial concentration, cAMP is gradually degraded since it is only produced at a low rate by Cyr1p and naturally degraded.

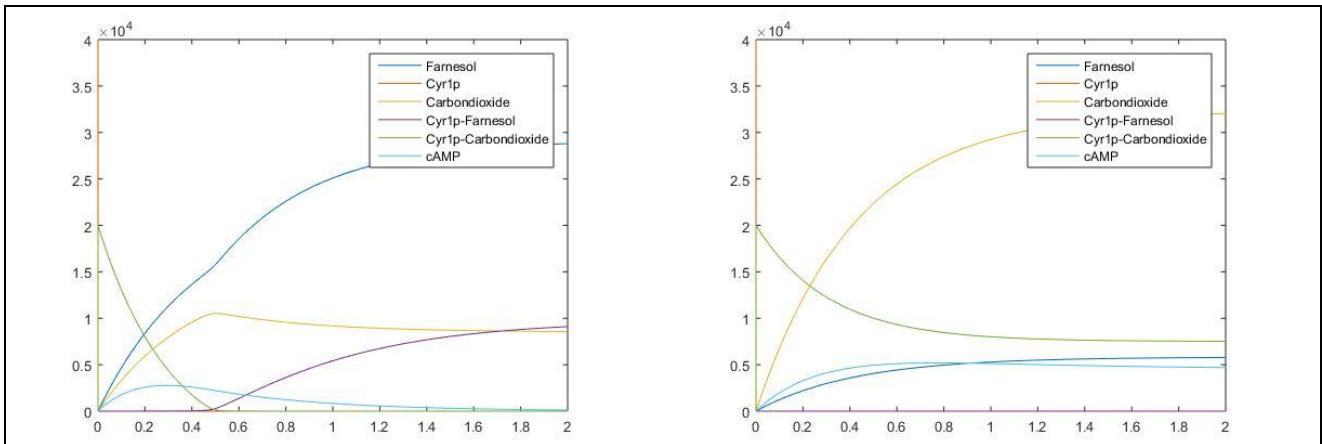


A. The simulation of Model 2 where all molecules are present. The chosen initial values are $F(0) = K(0) = 20000$ and $C(0) = 40000$ with the default parameter values listed in Table 2.



B. The simulation of Model 2 where all molecules are present. The chosen initial values are $F(0) = K(0) = 20000$ and $C(0) = 40000$ with $h = 7 \times 10^{-1}$ and other default parameter values listed in Table 2.

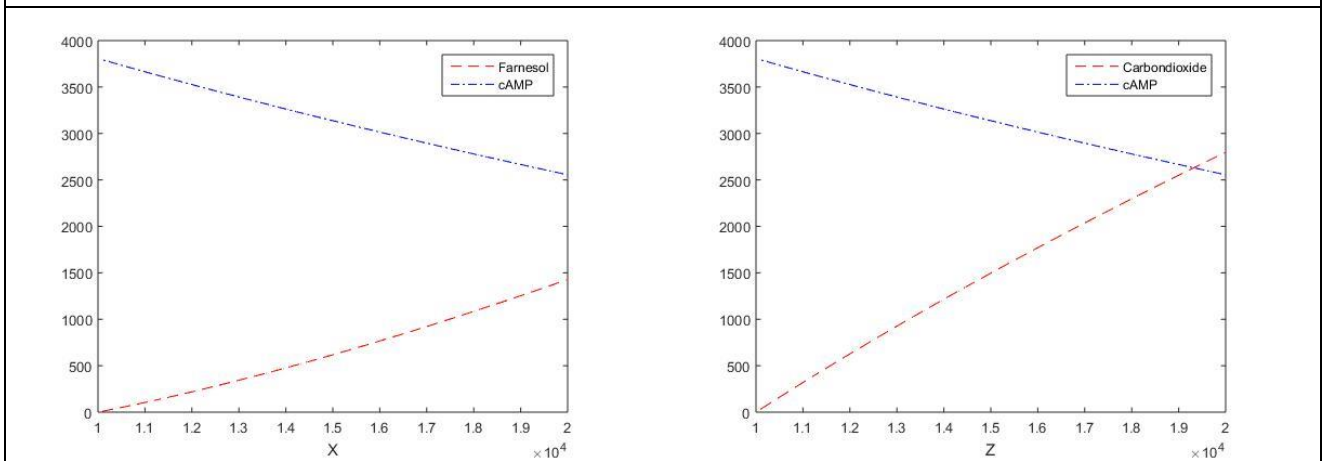
Figure 10: We can observe similar behaviors in Figures 10A and 10B, only that in Figure 10A, Cyr1p~Farnesol lasts a bit longer in the system since in Figure 10B, we set h , the rate at which Cyr1p~Farnesol triggers the dissociation of Cyr1p~CO₂, much larger than the default value. In both Figures 10A and 10B, we can observe that cAMP has a higher concentration than farnesol and Cyr1p~Farnesol. Moreover, Cyr1p~CO₂ maintains the highest concentration, which means that the molecule can still produce cAMP.



A. The simulation of Model 2 where all molecules are present. The chosen initial values are $F(0) = K(0) = 20000$ and $C(0) = 40000$ with $X = 10^5$, $h = 7 \times 10^{-1}$ and other default parameter values listed in Table 2.

B. The simulation of Model 2 where all molecules are present. The chosen initial values are $F(0) = K(0) = 20000$ and $C(0) = 40000$ with $Z = 10^5$, $h = 7 \times 10^{-1}$ and other default parameter values listed in Table 2.

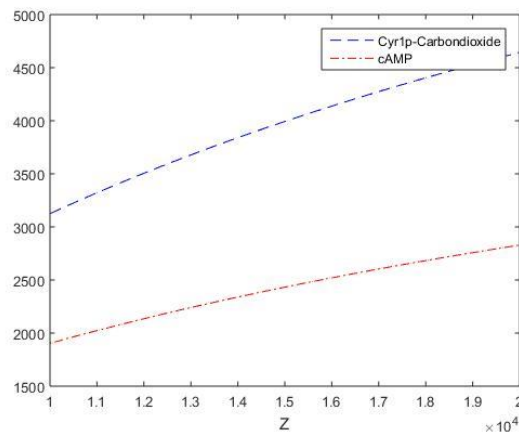
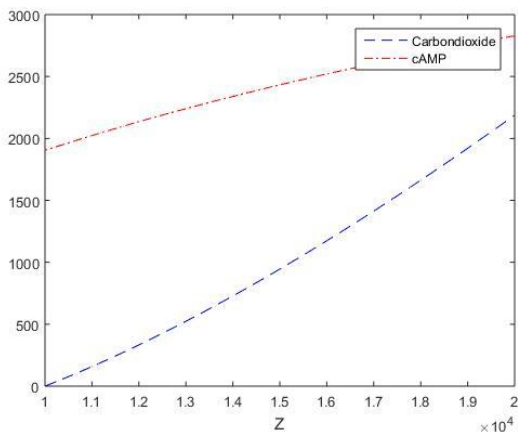
Figure 11: In Figure 11A, we set X , the production rate of farnesol, much larger than its default value. Since X is big, we can observe that farnesol has a very high concentration, which means it will produce more Cyr1p~Farnesol. Cyr1p~Farnesol triggers the dissociation of Cyr1p~CO₂ and gets used up quickly, but when Cyr1p~CO₂ falls low, Cyr1p~Farnesol gradually increases. Since Cyr1p and Cyr1p~CO₂ fall to very low concentrations, cAMP will also gradually decrease since its production agents are no longer present. On the other hand, in Figure 11B where we set Z , the production rate of CO₂, much larger than its default value, we can observe that CO₂ has a very high concentration. Moreover, we can also observe that Cyr1p and Cyr1p~Farnesol get used up very quickly. We can see that cAMP already has a high concentration, but Cyr1p~CO₂ has an even higher one, indicating that cAMP production will continue.



A. The relationships of X with farnesol and cAMP under default parameter values at steady state.

B. The relationships of Z with CO₂ and cAMP under default parameter values at steady state.

Figure 12: Figure 12A shows the relationships of X with farnesol and cAMP. As X increases, the amount of farnesol also increases since X is the key parameter determining farnesol concentration. On the contrary, cAMP decreases. In Figure 12B, we can observe that as Z increases, the amount of CO₂ also increases and therefore, the amount of cAMP should also increase since more CO₂ will form Cyr1p~CO₂, the main agent of cAMP production. However, Figure 12B shows that as Z increases, cAMP slowly decreases. This indicates that the mechanism in Model 2, in which farnesol targets Cyr1p~CO₂ by triggering its dissociation through Cyr1p~Farnesol, is more effective in inhibiting the cAMP pathway because even when Z and CO₂ increase, cAMP still decreases.



A. The relationships of Z with CO_2 and cAMP with $h = g = 10^{-10}$ and other default parameter values at steady state.

B. The relationships of Z with Cyr1p- CO_2 and cAMP with $h = g = 10^{-10}$ and other default parameter values at steady state.

Figure 13: Figure 13A shows the relationships of Z with CO_2 and cAMP with $h = g$. As Z increases, the amounts of CO_2 and cAMP also increase. In Figure 13B we illustrate the relationships of Z with Cyr1p- CO_2 and cAMP. As Z increases, the amounts of Cyr1p- CO_2 and cAMP also increase.

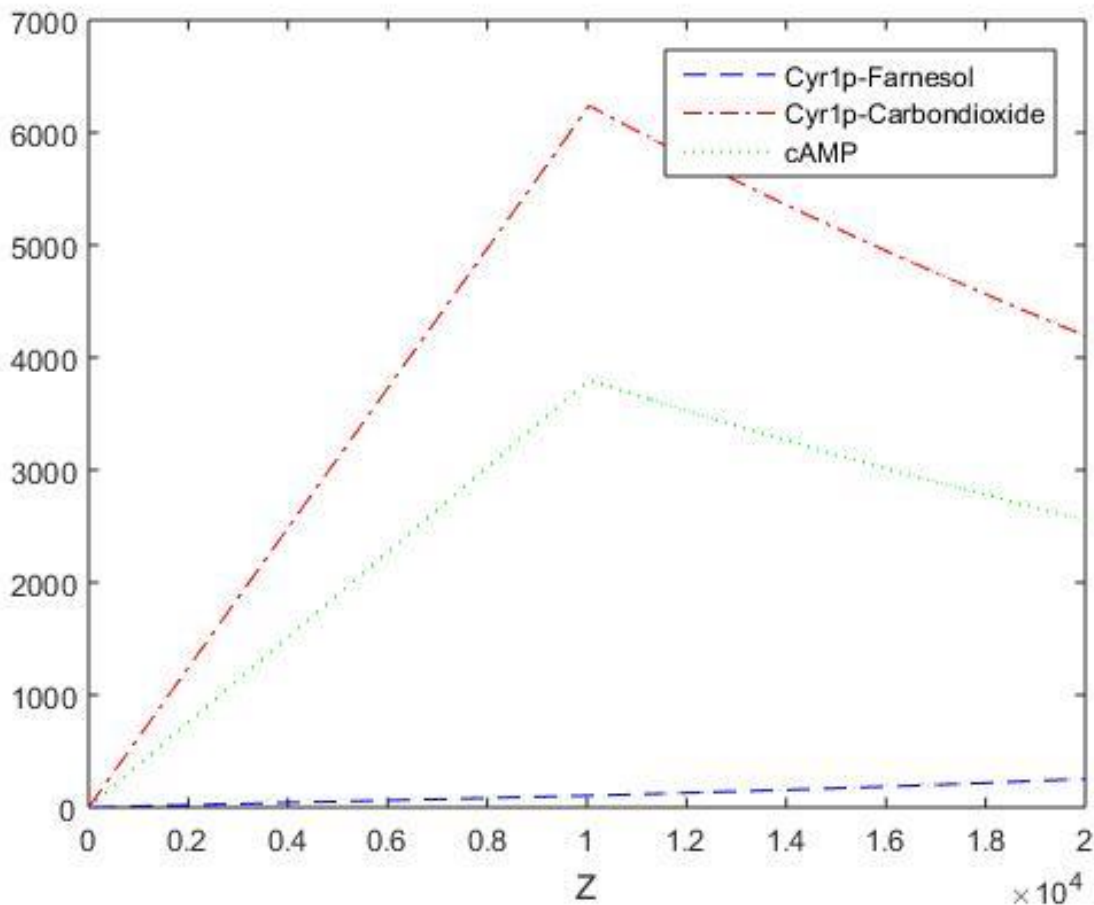
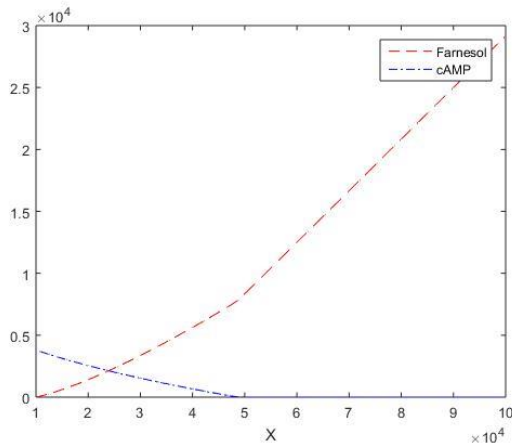
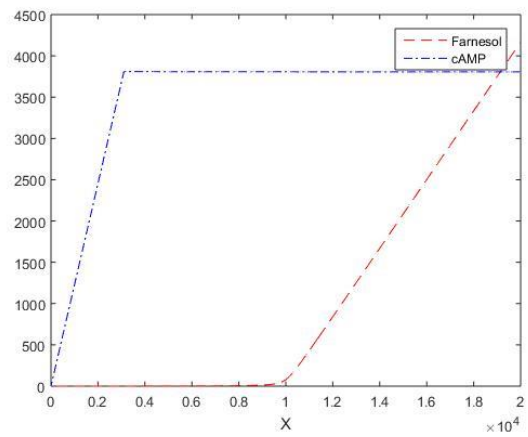


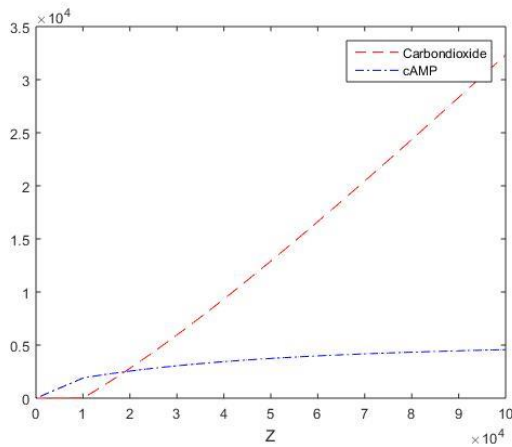
Figure 14: The simulation illustrating the relationships of Z with Cyr1p-Farnesol, Cyr1p- CO_2 and cAMP at steady state. Figure 14 shows that as Z increases, initially cAMP and Cyr1p- CO_2 increase as well while Cyr1p-Farnesol stays low. However, when Cyr1p-Farnesol starts to increase as Z also increases, both cAMP and Cyr1p- CO_2 start decreasing because Cyr1p-Farnesol will promote the dissociation of Cyr1p- CO_2 so this complex cannot produce cAMP at a high rate.



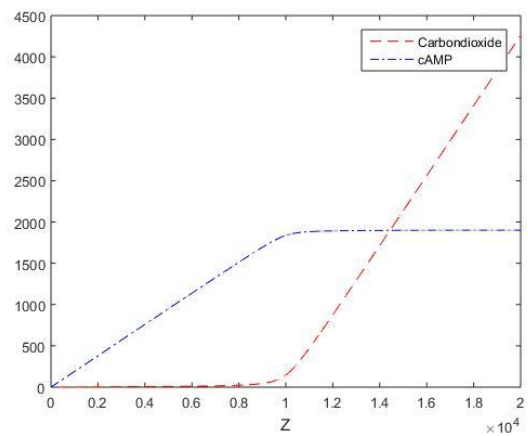
A. The relationships of X with farnesol and cAMP when $h = 2.7$ and $X = 10^5$ at steady state.



B. The relationships of X with farnesol and cAMP when $h = 2.7$ and $a = 1.1$ at steady state.



C. The relationships of Z with CO₂ and cAMP when $h = 2.7$ and $Z = 10^5$ at steady state.



D. The relationships of Z with CO₂ and cAMP when $h = 2.7$ and $d = 1$ at steady state.

Figure 15: In Figure 15A, we make h and X much bigger than the default values which automatically result in high concentrations of both farnesol and Cyr1p~Farnesol. We can observe that cAMP gets degraded very quickly. Moreover, Figure 15A shows that farnesol increases more rapidly as cAMP gets degraded completely. In Figure 15B, we increase h and reduce a , the binding rate of farnesol and Cyr1p. This setting gives an increase of cAMP concentration and a constant farnesol concentration at first, but then farnesol starts to increase as X increases, making cAMP stay constant since more Cyr1p~Farnesol will be produced if farnesol increases and therefore more Cyr1p~CO₂ will dissociate and cAMP cannot be produced at a high rate. In Figure 15C, we illustrate the relationships of Z with CO₂ and cAMP. As Z increases, the amount of CO₂ also quickly increases. However, the amount of cAMP increases very slowly because h is still much larger than the default value. In Figure 15D, we set d , the binding rate of Cyr1p and CO₂, much smaller than the default value. Under this setting, as Z increases, CO₂ takes time to finally increase after staying constant. cAMP immediately increases, since d is very small so it is solely produced by Cyr1p and even though h is large, Cyr1p~Farnesol does not directly target cAMP molecules. However, when CO₂ finally increases, cAMP suddenly stays constant because at this point, more Cyr1p~CO₂ will be produced and dissociate again since h is large.

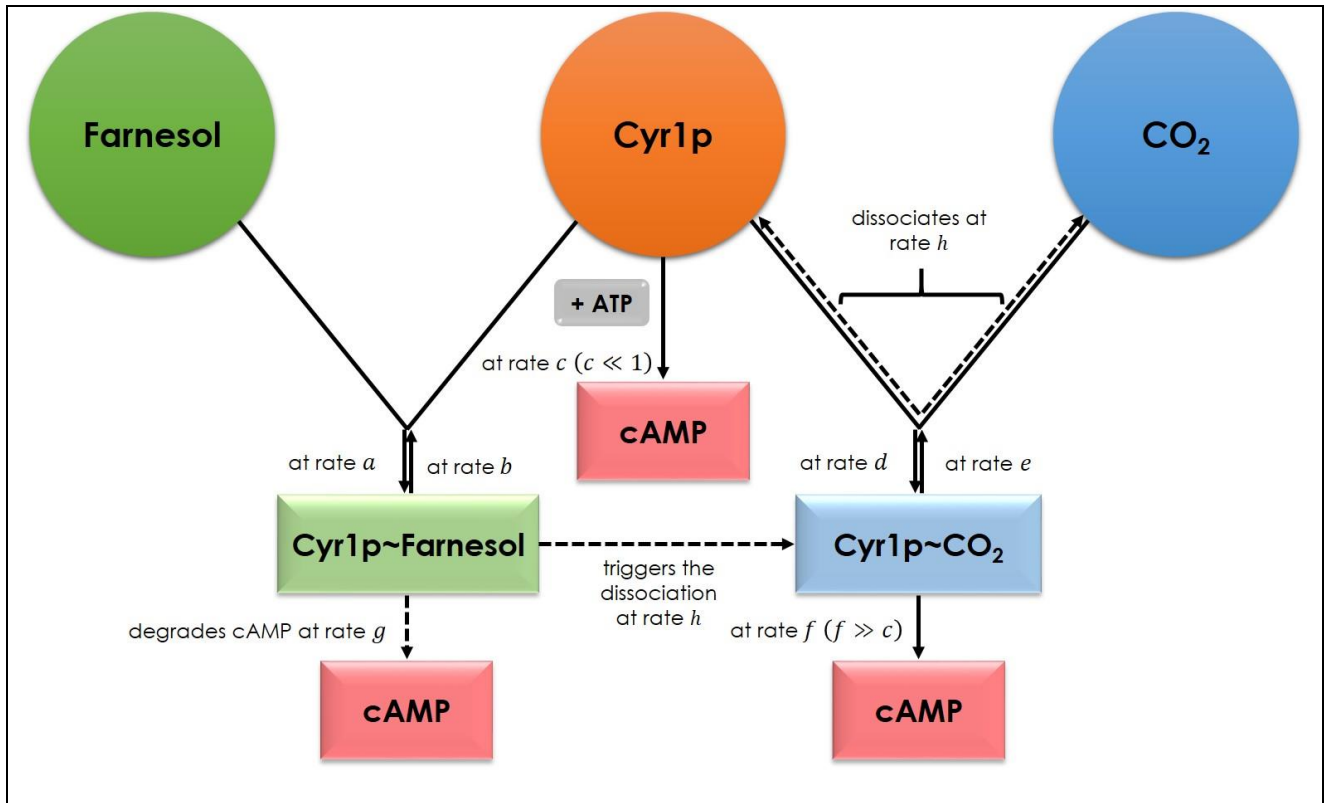


Figure 16: Another possible scenario at which both mechanisms that we have proposed previously happen simultaneously in one system. Here, farnesol binds to Cyr1p at rate a forming the complex Cyr1p~Farnesol, which degrades cAMP directly at rate g and also triggers the dissociation of the complex formed from the binding of Cyr1p and CO₂, Cyr1p~CO₂, at rate h . Cyr1p can produce cAMP by changing ATP molecules into cAMP molecules at rate c , and bind to CO₂ at rate d , forming the complex Cyr1p~CO₂. Both complexes, Cyr1p~Farnesol and Cyr1p~CO₂, can dissociate at rates b and e respectively. Moreover, the complex Cyr1p~CO₂ can produce cAMP molecules at rate f .